Available online at www.sciencedirect.com
ScienceDirect
Journal of Nuclear Materials 363–365 (2007) 550–554
journal of nuclear materials
www.elsevier.com/locate/jnucmat

Control of test particle transport in a turbulent electrostatic model of the Scrape-Off-Layer

G. Ciraolo [a,*], Ph. Ghendrih [b], Y. Sarazin [b], C. Chandre [c], R. Lima [c], M. Vittot [c], M. Pettini [d]

[a] *Ecole Centrale de Marseille and MSNM-GP Unité Mixte de Recherche (UMR 6181) du CNRS, Technopole de Château, Gombert F-13451, France*
[b] *Association Euratom-CEA, DRFC/DSM/CEA, CEA Cadarache, F-13108 St. Paul-lez-Durance Cedex, France*
[c] *Centre de Physique Théorique, CNRS Luminy, Case 907, F-13288 Marseille Cedex 9, France*[1]
[d] *Instituto Nazionale di Astrofisica, Osservatorio di Arcetri, Largo Enrico Fermi 5, I-50125 Firenze, Italy, and INFN Sezione di Firenze, Firenze, Italy*

Abstract

The $\boldsymbol{E}\times\boldsymbol{B}$ drift motion of charged test particle dynamics in the Scrape-Off-Layer (SOL) is analyzed to investigate a transport control strategy based on Hamiltonian dynamics. We model SOL turbulence using a 2D non-linear fluid code based on interchange instability which was found to exhibit intermittent dynamics of the particle flux. The effect of a small and appropriate modification of the turbulent electric potential is studied with respect to the chaotic diffusion of test particle dynamics. Over a significant range in the magnitude of the turbulent electrostatic field, a three-fold reduction of the test particle diffusion coefficient is achieved.

PACS: 05.45.Gg; 52.25.Fi; 52.25.Xz; 52.35.Ra; 47.27.Rc

Keywords: Turbulence; Control; Passive tracers; Nonlinear dynamics

1. Introduction

Cross-field turbulent transport in the Scrape-Off-Layer (SOL) has a strong influence on divertor efficiency and thus on the overall performance of discharges. Recent experiments as well as numerical investigations suggest a non-diffusive transport in the SOL. The transport seems to be characterized by large intermittent events which propagate ballistically with large velocities. On the one hand SOL turbulence can cross H-mode barrier and connect SOL and core turbulence, destabilizing the pedestal stable region. On the other hand, when large intermittent events propagate in the far SOL, they can modify the recycling pattern and consequently the wall particle content and thus the wall tritium inventory. Furthermore, such a convection of hot ion

* Corresponding author.
E-mail address: guido.ciraolo@l3m.univ-mrs.fr (G. Ciraolo).
[1] Unité Mixte de Recherche (UMR 6207) du CNRS, et des universités Aix-Marseille I, Aix-Marseille II et du Sud Toulon-Var. Laboratoire affilié à la FRUMAM (FR 2291). Laboratoire de Recherche Conventionné du CEA (DSM-06-35).

0022-3115/$ - see front matter
doi:10.1016/j.jnucmat.2006.12.030

over-densities can lead to localised heat deposition on components that are not designed to sustain meaningful plasma energy deposition. A strategy to control intermittent transport can therefore prove to be highly valuable to achieve high performance operation.

Several experiments [1,2] have been dedicated to the control of turbulence in magnetized plasmas. Although a modelling of some of the experiments has been achieved, there was to date no theoretical backing for such a procedure. Our aim is to develop such a theoretical background and proceed by steps towards a realistic turbulence control scheme. In the present paper, we apply the control strategy derived for Hamiltonian systems to the transport of test particles in an electrostatic potential which exhibits key features of the turbulent electrostatic potential generated by the Tokam code. This is a 2D non-linear fluid code based on interchange instability [3,4].

The investigation of passive tracer dynamics has demonstrated to be a powerful tool for a deeper understanding of fluid and plasma turbulence, even if, in the case of plasmas, one has to be cautious about the limits of its applicability due to the back-reaction of turbulence on electro-magnetic fields [5–8].

Our strategy is to define a small apt modification of the system which enhances confinement, at low additional cost of energy [9–11]. In the present case it consists in reducing the chaotic diffusion of charged test particles advected by the $\boldsymbol{E}\times\boldsymbol{B}$ drift motion. This effect is obtained by adding a small control term to the turbulent electric potential and comparing the chaotic diffusion of the test particles advected by the original electric potential and by the modified one.

In the case of turbulence with intermittent bursts of transport, one has to specify the control strategy: Either one aims at controlling turbulence in between the bursts of transport with a fluctuation level of the order of 2%, or one aims at controlling the intermittent events with fluctuation levels larger than 10%. The former is comparable to the case of homogeneous turbulence and is readily achieved while the latter is more challenging and is presently investigated.

The paper is organized as follows. In Section 2 the 2D model for SOL turbulence is recalled as well as its non-linear transport properties. In Section 3 the procedure for the computation of the control term is described and the results of its application to the $\boldsymbol{E}\times\boldsymbol{B}$ drift motion of charged test particles are presented.

2. Interchange turbulence in the Scrape-Off-Layer

SOL turbulence is specific with respect to core turbulence due to the sheath boundary conditions that strongly reduce the parallel current flowing on each flux tube. Regimes with reduced parallel current are then very sensitive to charge separation via the curvature drift since the parallel current is less effective to balance the charge separation. In fact, the interchange instability, hence curvature charge separation combined to a density gradient, in conjunction with the sheath resistivity have been proposed to explain the very large fluctuation levels reported in the SOL [12,13]. We consider here this model of SOL turbulence in the limit $T_i \ll T_e$. In this model two balance equations are used, the particle balance that governs the density transport, and the charge balance which takes the form of an evolution equation for the vorticity $\Delta\phi$, where ϕ is the electric potential, due to the ion inertia terms. Further simplifications are introduced in the flute limit, hence with weak parallel gradients such that the average along the field lines can be performed. The system is thus reduced to a two dimensional and two field model, n the density and ϕ the plasma potential normalised to T_e/e, given by

$$\begin{aligned}&\left(\frac{\partial}{\partial t} - D\nabla_\perp^2 + \{\phi\}\right)n = \sigma_n n + S,\\ &n\left(\frac{\partial}{\partial t} - \nu\nabla_\perp^2 + \{\phi\}\right)\nabla_\perp^2\phi + g\partial_y n = \sigma_\phi n.\end{aligned} \tag{1}$$

In these equations time is normalised to the ion Larmor frequency Ω_i and space is normalised to the so-called hybrid Larmor radius ρ_s. D and ν stand for the collisional transverse diffusion and viscosity (normalised to the Bohm values), S is the density source term, here localised radially and constant in time and along the poloidal angle θ. σ_n and σ_ϕ are the sheath controlled particle flux and current to the wall, $\sigma_n = \sigma\exp(\Lambda - \phi)$ and $\sigma_\phi = \sigma(1 - \exp(\Lambda - \phi))$ where $\sigma = \rho_s/qR$ stands for the normalised saturation current. The operator $\{\phi\}F = \{\phi, F\} = \partial_x\phi\partial_y F - \partial_y\phi\partial_x F$ is the electric drift convection term. At first order in the fluctuation magnitude, sheath loss terms can be linearised to yield the Hasegawa–Wakatani coupling term $\sigma(n - \phi)$ [14]. The interested reader can refer to Refs. [3,4] for more details in Eq. (1), the assumptions of this model and its transport properties.

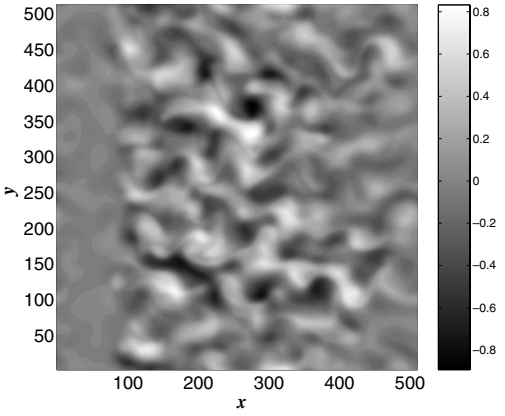

Fig. 1. Snapshot of the electric potential $\phi(x,y,t)$ for $t=100$ obtained by Eq. (1) on a spatial grid of $512\,\rho_s \times 512\,\rho_s$.

Large systems with $512\,\rho_s$ in both the radial and poloidal directions are simulated for about 200 SOL confinement times (typically 1500 turbulence correlation times). A localised particle source, with Gaussian shape in the radial direction and width $8.5\,\rho_s$ and no dependence in poloidal angle or time, splits the box in two regions, an unstable region where the average density gradient is negative and exceeds the threshold of the interchange turbulence, and a stable region with positive gradient of the average density and where the system is stable with respect to the interchange mechanism. A contour plot of the electric potential at a given time is shown in Fig. 1. Typical power spectra of the potential in the x and y direction are shown in Fig. 2.

In the following Section we study the effect of the control term on $\boldsymbol{E}\times\boldsymbol{B}$ drift motion of charged test particles.

3. Turbulent potential and test particle dynamics

In the guiding center approximation, the equations of motion of a charged test particle in presence of a strong toroidal magnetic field and of a time dependent electric field are [15]:

$$\dot{\mathbf{x}} = \frac{\mathrm{d}}{\mathrm{d}t}\begin{pmatrix} x \\ y \end{pmatrix} = \frac{c}{B^2}\mathbf{E}(\mathbf{x},t)\times\mathbf{B} = \frac{c}{B}\begin{pmatrix} -\partial_y\phi(x,y,t) \\ \partial_x\phi(x,y,t) \end{pmatrix}, \tag{2}$$

where ϕ is the electric potential, $\mathbf{E}=-\nabla\phi$, and $\mathbf{B}=B\mathbf{e}_z$. We study the 2D dynamics of test particles obeying to Eq. (2), where the considered turbulent potential is generated by Eq. (1). We consider a reduced selected spatial region and we impose periodic boundary conditions in x, y directions. More precisely we choose a square box of $256\,\rho_s \times 256\,\rho_s$, not too close to the source region (in Fig. 1 the selected square box is between $x\in[100,356]$ in the radial direction and $y\in[1,256]$ in the poloidal direction). This allows one to avoid the complex analysis of diffusive transport in finite systems, namely where the sources and sinks play an important role. With such an infinite system, one can use a straightforward calculation of diffusion coefficients to characterize the turbulent transport. Since we are interested in long time behaviour of test particle dynamics, we impose periodic boundary conditions also in time. Periodicity in time provides a means to generate appropriate statistics with long time series. The underlying assumption is that all meaningful time scales of the system are shorter than the chosen period. A snapshot of the turbulent potential in the selected spatial region after the filtering procedure

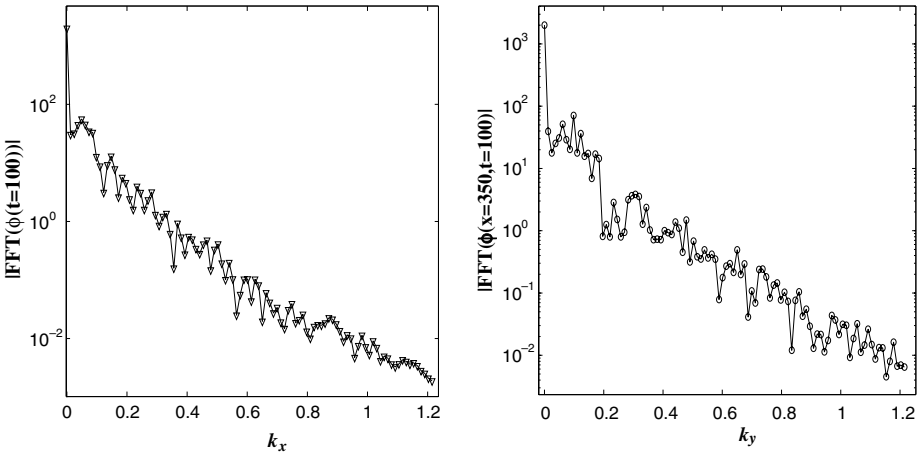

Fig. 2. Typical power spectra of the electric potential ϕ represented in Fig. 1 at $t=100$ using the same parameter as in Fig. 1.

for imposing periodic boundary conditions is shown in Fig. 3. In what follows we denote $V(x,y,t)$ the filtered potential. Therefore the potential $V(x,y,t)$ is $L_x = 256\rho_s$ periodic in the x-direction, $L_y = 256\rho_s$ periodic in the y-direction and $T = 256 \times 50\Omega_i^{-1}$ periodic in time.

In order to have a 1-periodic dependence in (x,y,t) for simplicity, we perform the change of variables

$$\tilde{x} = \frac{x}{L_x}, \quad \tilde{y} = \frac{y}{L_y}, \quad \tilde{t} = \frac{t}{T}. \tag{3}$$

It follows that

$$\frac{\mathrm{d}\tilde{x}}{\mathrm{d}\tilde{t}} = \frac{T}{L_x}\frac{\mathrm{d}x}{\mathrm{d}t} = -\frac{T}{L_x}\frac{\partial V}{\partial y}. \tag{4}$$

From

$$\frac{\partial V}{\partial y} = \frac{\partial V}{\partial \tilde{y}}\frac{\mathrm{d}\tilde{y}}{\mathrm{d}y}, \tag{5}$$

we get

$$\frac{\mathrm{d}\tilde{x}}{\mathrm{d}\tilde{t}} = -\frac{T}{L_x L_y}\frac{\partial \tilde{V}(\tilde{x},\tilde{y},\tilde{t})}{\partial \tilde{y}}. \tag{6}$$

Thus the equations in the $(\tilde{x},\tilde{y},\tilde{t})$ variables are equivalent to the equations in the (x,y,t) variables if the potential is multiplied by a factor $\frac{T}{L_x L_y}$.

The test particle dynamics governed by Eq. (2) is studied with the aid of numerical simulations. Since the potential is given over a spatio-temporal grid, the estimation of the electric field which acts on the particle trajectories is computed using a four point bivariate interpolation in space and a linear interpolation in time [16]. The time integration is performed using a fourth order Runge–Kutta scheme.

We consider a set of M particles (M of order 1000) uniformly distributed at random at $t = 0$ and we study the diffusion properties of the system. We verified that for the values of the parameters in the range of interest the mean square displacement $\langle r^2(t)\rangle$ is a linear function of time and we computed the corresponding diffusion coefficient

$$D^\star = \lim_{t\to\infty}\frac{\langle r^2(t)\rangle}{t},$$

as a function of the amplitude of the turbulent potential. In Fig. 4 the results obtained for small values of the electric potential are shown.

The first step in the computation of the appropriate modification of the potential which entails a reduction of chaotic diffusion is the Fourier expansion of the electric potential, i.e.,

$$V(x,y,t) = \sum_{k_1,k_2,k_3} V_{k_1k_2k_3}\mathrm{e}^{2\pi i(k_1x+k_2y+k_3t)}. \tag{7}$$

Then we compute ΓV, that is the time-integral of V,

$$\Gamma V = \sum_{k_1,k_2,k_3\neq 0}\frac{V_{k_1k_2k_3}}{2\pi i k_3}\mathrm{e}^{2\pi i(k_1x+k_2y+k_3t)}, \tag{8}$$

and the constant part of V with respect to time that is written $\mathscr{R}V$:

$$\mathscr{R}V = \sum_{k_1,k_2} V_{k_1k_20}\mathrm{e}^{2\pi i(k_1x+k_2y)}. \tag{9}$$

The control term f_2 is given by the Poisson bracket between ΓV and $(\mathscr{R}+1)V$,

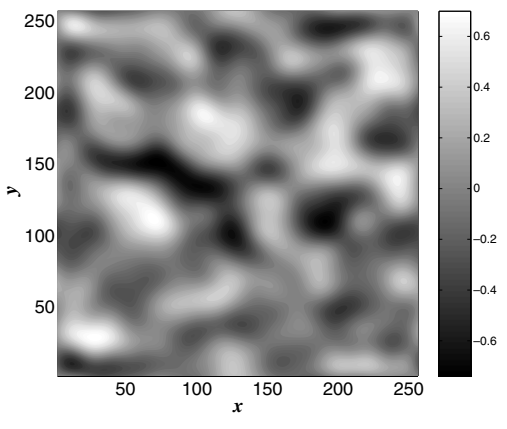

Fig. 3. Snapshot of the electric potential $V(x,y,t)$ for $t = 100$ over the spatial grid of $256\rho_s \times 256\rho_s$ obtained from the original potential ϕ represented in Fig. 1 after the filtering in space and time.

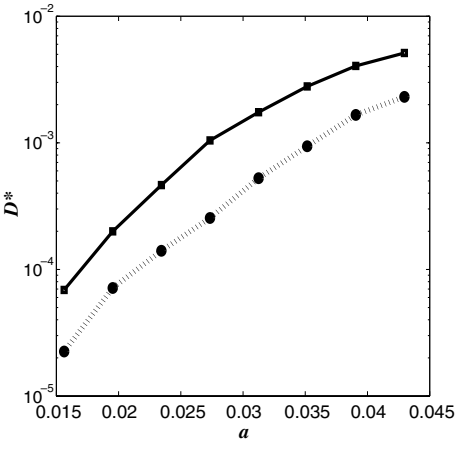

Fig. 4. Test particle diffusion coefficient $D^\star$ versus a (magnitude of the potential) in log–lin scale obtained for the turbulent potential V without (full squares, solid line) and with (full circles, dashed line) the addition of the control term f_2 given by Eq. (10).

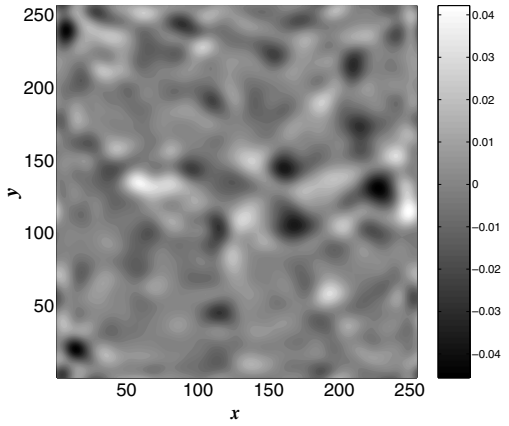

Fig. 5. Contour plot of the control term $f_2(x,y,t)$ for $t=100$ given by Eq. (10).

$$f_2 = -\frac{1}{2}\{\Gamma V,(\mathscr{R}+1)V\} = -\frac{1}{2}\left(\frac{\partial \Gamma V}{\partial x}\frac{\partial(\mathscr{R}+1)V}{\partial y} - \frac{\partial \Gamma V}{\partial y}\frac{\partial(\mathscr{R}+1)V}{\partial x}\right). \tag{10}$$

A contour plot of f_2 at a fixed time is depicted in Fig. 5. Finally we study the test particle dynamics in the modified potential $V+f_2$. The comparison between the diffusion coefficient obtained with and without the control term is shown in Fig. 4. One readily observes two main features, on the one hand the control term exhibits higher frequencies than the turbulent electrostatic field, typically a factor 2 larger as expected from the quadratic form of the control term given by Eq. (10). On the other hand the magnitude of the control term is more than a factor 10 smaller. This reduction compensates for the increase of the electric field via the increased frequencies. A significant reduction of $D^{\star}$ is observed in the controlled case. These preliminary results obtained for small amplitudes of the electric potential show that the control strategy we propose can be applied to much more turbulent flows than the one considered in [9]. Further investigations on the efficiency domain of the control term and its robustness are required.

4. Discussion and conclusion

In this paper, we have shown that the procedure developed to control turbulent diffusive transport of test particles can be applied to particles transported in a realistic turbulent electrostatic potential. The procedure to compute a low magnitude control term provides an efficient turbulence reduction. For this test of the control strategy the turbulent field is truncated to simplify the analysis of test particle transport. More generally, the proof of principle that a control strategy can be efficient is tested on the simplest available model. When comparing the diffusion coefficient of the test particles in the uncontrolled system to that in the controlled case, a typical factor 3 reduction of the diffusion coefficient is achieved with a factor 10 lower magnitude of the control term. Far more investigation is still required on the way towards realistic control systems for the turbulent transport. However, the present paper shows that a theory based starting point is available.

References

[1] C. Schröder, T. Klinger, D. Block, A. Piel, G. Bonhomme, V. Naulin, Phys. Rev. Lett. 86 (2001) 5711.
[2] J. Stöckel et al., Plasma Phys. Control. Fusion 47 (2005) 635.
[3] Y. Sarazin, Ph. Ghendrih, Phys. Plasmas 5 (1998) 4214.
[4] Ph. Ghendrih et al., Nucl. Fusion 43 (2003) 1013.
[5] V. Naulin, O.E. Garcia, M. Priego, J. Juul Rasmussen, Phys. Scr. T 122 (2006) 129.
[6] V. Naulin, Phys. Rev. E 71 (2005) 015402.
[7] M. Priego, O.E. Garcia, V. Naulin, J. Juul Rasmussen, Phys. Plasmas 12 (2005) 062312.
[8] R. Basu, V. Naulin, J. Juul Rasmussen, Commun. Nonlinear Sci. Numer. Simul. 8 (2003) 477.
[9] G. Ciraolo et al., Phys. Rev. E 69 (2004) 056213.
[10] C. Chandre et al., Phys. Rev. Lett. 94 (2005) 074101.
[11] C. Chandre, M. Vittot, G. Ciraolo, Ph. Ghendrih, R. Lima, Nucl. Fusion 46 (2006) 33.
[12] A.V. Nedospasov, Sov. J. Plasma Phys. 15 (2003) 659.
[13] X. Garbet et al., Nucl. Fusion 31 (1991) 967.
[14] M. Wakatani, A. Hasegawa, Phys. Fluids 27 (1984) 611.
[15] T.J. Northrop, Ann. Phys. 15 (1961) 79.
[16] M. Abramowitz, I.A. Stegun, Handbook of Mathematical functions, Dover Publications, 1970.